How Should Climate Change Uncertainty Impact Social Valuation and Policy?

Michael Barnett (ASU) William A. Brock (Wisconsin)
Lars Peter Hansen (University of Chicago)

December 9, 2020

Abstract

The design and conduct of climate change policy necessarily confronts uncertainty along multiple fronts. We explore the consequence of ambiguity over various sources and configurations of models that impact how economic opportunities could be damaged in the future. We take inventory of three alternative sources of uncertainty and provide a novel way to assess it. These include i) *carbon dynamics* that capture how carbon emissions impact atmospheric carbon in future time periods; ii) *temperature dynamics* that depict how atmospheric carbon alters temperature in future time periods; iii) *damage functions* that quantify how temperature changes diminish economic opportunities. We show how uncertainty sources interact for a social planner looking to design a prudent approach to the social pricing of carbon emissions. Our uncertainty decompositions, which are disciplined by quantitative geoscientific modeling of the first two channels and quantitative economic modelling of the third, provide guidance to where resources should be allocated towards uncertainty reduction. Decision theory under ambiguity provides a framework for our economically motivated approach to uncertainty quantification.

1 Introduction

There are many calls for policy implementation to address climate change based on confidence in our knowledge of the adverse impact of economic activity on the climate and conversely. Given a mature understanding of the coupled climate–economy dynamics, arguably we should be directing scholarly endeavors to support concrete and viable proposals for collective action, (e.g., the Nordhaus, 2015 "Climate Clubs") and advocacy for implementation. The perspective we embrace is different. Our view is that the knowledge base remains incomplete, and it is important to acknowledge and account for the remaining uncertainties when exploring prudent approaches to climate policy.

We are not alone in this view. In climate economics, Weitzman (2012), Wagner and Weitzman (2015) and others have emphasized uncertainty in the climate system's dynamics and how this uncertainty could create fat-tailed distributions of potential damages. Relatedly, Pindyck (2013) and Morgan et al. (2017) find existing integrated assessment models in climate economics to be of little value in the actual prudent policy. While we share these concerns, our aim is to explore ways to incorporate uncertainty explicitly into policy discussions. Not only is there substantial uncertainty about the economic inputs but also about the geoscientific inputs.

Barnett et al. (2020) proposed a framework for assessing uncertainty, broadly-conceived, to include ambiguity over alternative models and potential model misspecification. In effect, they suggest methods for conducting structured uncertainty analyses. But like the entire literature, their examples scratch the surface of the actual quantitative assessment of uncertainty pertinent to the problem of climate change.

We suggest two alternative ways to view our approach to uncertainty. Under one view, a decision maker, in this case a fictitious social planner, faces a tradeoff between projecting the "best guess" consequences of alternative courses of action versus "worst possible" outcomes among a well defined set of alternative models. Rather than focusing exclusively on these extremal points, we allow our decision maker to take intermediate positions in accordance with an ambiguity aversion parameter. Under a complementary view, a decision maker confronts many dimensions of uncertainty and engages in a sensitivity analysis. For instance, in this paper we consider up to 459 different model configurations with uncertainty about how to weight them as in robust Bayesian analyses. We use the social planner's decision problem to add structure to this sensitivity analysis and reduce a potentially high-dimensional sensitivity analysis to a one-dimensional characterization of sensitivity captured by a scalar ambiguity aversion parameter.

This paper takes inventory of the consequence of alternative sources of uncertainty and provides a novel way to assess it, We consider three:

- *carbon dynamics* mapping from carbon emissions to carbon in the atmosphere
- *temperature dynamics* mapping from carbon in the atmosphere to temperature changes
- *economic damages* what fraction of the productive capacity is destroyed by temperature changes

We necessarily adopt some stark simplifications to make this analysis tractable. Many of the climate models are of both high dimension and highly nonlinear. Rather than using those models directly, we rely on outcomes of pulse experiments applied to the models. We then take the outcomes of these pulse experiments as inputs into our climate economic model. We follow much of the environmental economics in the use of *ad hoc* static damage functions, and explore the consequences of changing the curvature in these damage functions. Even with these simplifications, our uncertainty analysis is sufficiently rich to show how alternative components of uncertainty interact in important ways.

We use the social cost of carbon (SCC) as a barometer for investigating the consequences of uncertainty for climate policy. In settings with uncertainty, as featured by Barnett et al., we depict this as an asset price. The social counterpart to a cash flow is the impulse response from a marginal increase in emissions to a marginal impact on the logarithm of damages. This cash flow is "discounted" stochastically in ways that account for uncertainty. This follows in part revealing discussions in Golosov et al. (2014) and Cai et al. (2017) who explore some of the risk consequences for the social cost of carbon. Barnett et al. take a broader perspective on uncertainty and show how to construct a change in probability measure to account for this uncertainty.

2 Uncertain climate dynamics

Joos et al. (2013) report the responses of atmospheric carbon concentration to emission pulses of one hundred gigatons of carbon for several alternative models. We use responses for nine such models.[1]

Geoffroy et al. (2013) approximates the temperature dynamics of seventeen different models using the following specification:

$$\begin{aligned} \mathsf{c}_s \frac{dT^s}{dt} &= F - \gamma T^s - \epsilon\chi(T^s - T^o) \\ \mathsf{c}_o \frac{dT^o}{dt} &= -\chi(T^o - T^s) \\ F &= 5.35\left(\log CO_2 - \log \underline{CO_2}\right) \end{aligned}$$

where T^s is the surface temperature, T^o is the ocean temperature, CO_2 is atmospheric carbon dioxide, and $\underline{CO_2}$ is the preindustrial benchmark. The construction of F comes from the "Arrhenius" equation. The parameters used in this simplified representation differ depending on the model used in the approximation. We use this specification along with Geoffroy et al.'s estimates of 17 such models in our simulations.[2]

We then take the nine different atmospheric carbon responses as inputs into these seventeen temperature dynamics approximations, giving us a total of 153 different temperature responses to carbon in the atmosphere. The resulting temperature responses are reported in the upper panel of Figure 1.

[1] Appendix A provides additional details and lists the specific models we use from Joos et al. (2013).

[2] Appendix A provides additional details and lists the specific models we use from Geoffroy et al. (2013).

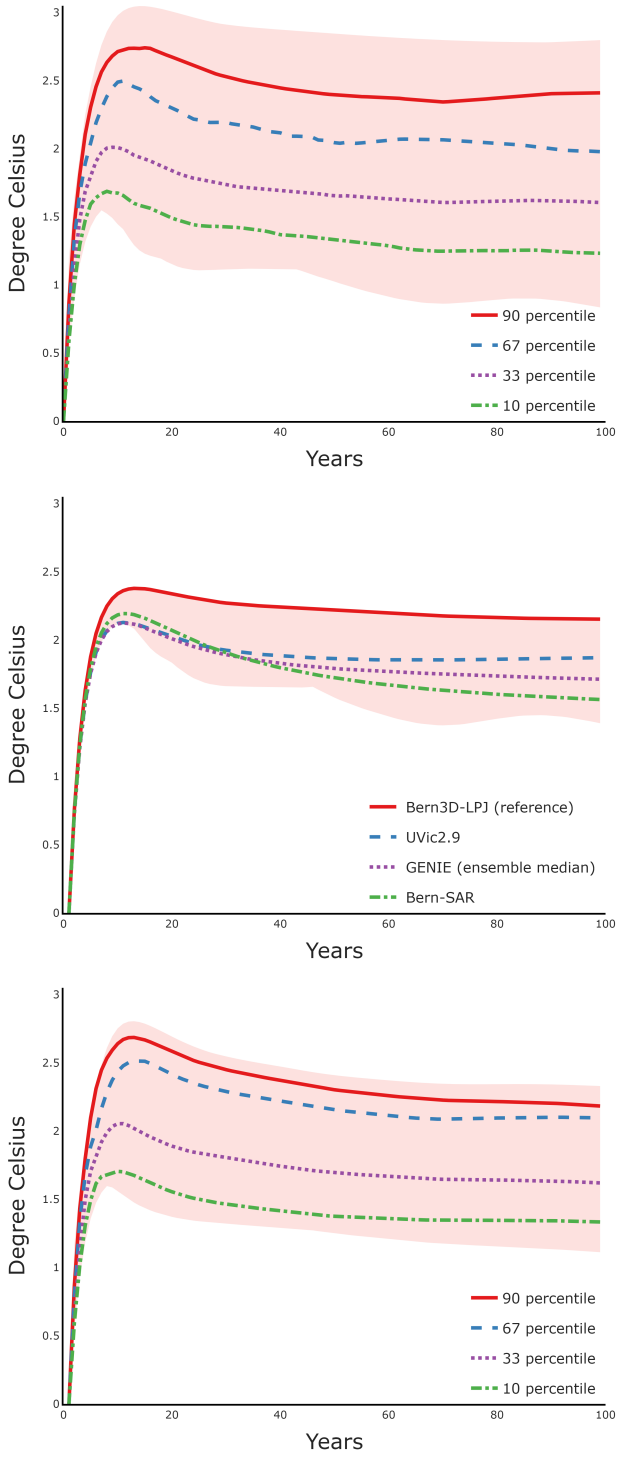

Figure 1: Percentiles for temperature responses to emission impulses. The emission pulse was 100 gigatons of carbon (GtC) spread over the first year. The temperature units for the vertical axis have been multiplied by ten to convert to degrees Celsius per teraton of carbon (TtC). The boundaries of the shaded regions are the upper and lower envelopes. Top panel: percentiles for impulse responses including both carbon and temperature uncertainty. Center panel: responses obtained for four of the temperature responses from the nine different carbon responses each averaged over the seventeen models of temperature dynamics. Bottom panel: percentiles for the seventeen temperature responses using each averaged over the nine models of carbon concentration dynamics.

Figure 1 captures the response patterns featured by Ricke and Caldeira (2014). The maximal temperature response to an emission pulse occurs at about a decade and the subsequent response is very flat. This figure also reports the percentiles for each horizon computed using the 153 different temperature response functions. While there are similar patterns across the temperature response functions, there is considerable heterogeneity in the magnitudes of the responses. For further characterization of this heterogeneity, we compute the exponentially weighted average of each of these response functions and report the resulting histogram in Figure 2.

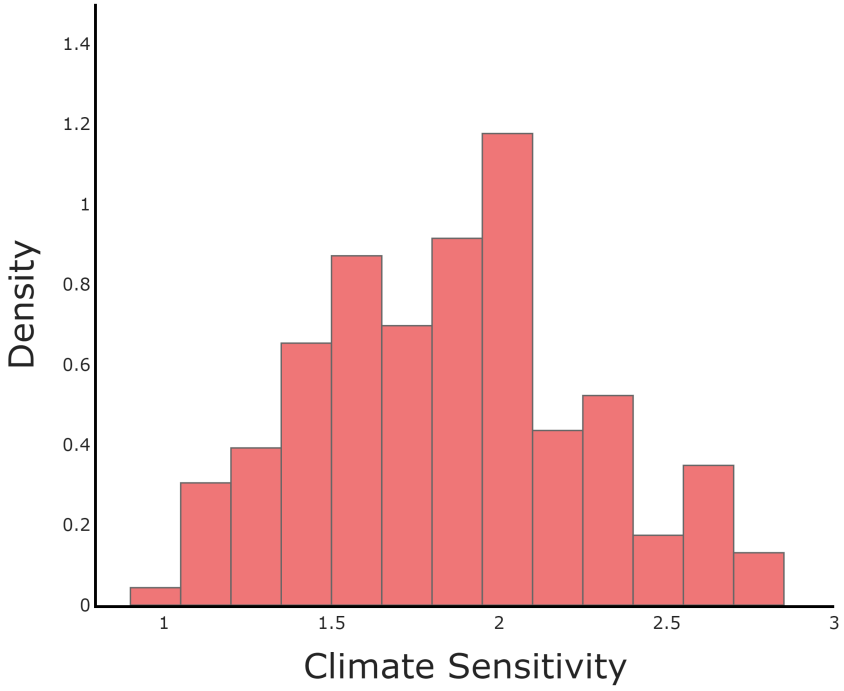

Figure 2: Histogram for the exponentially weighted responses of temperature to an emissions impulse from 153 different models where the weights are discounted using a rate $\delta = .01$.

The eventually flat trajectories of the temperature response functions are consistent with model comparisons made using what is called the transient climate response (TCRE) to CO_2 emissions. The TCRE is the ratio of CO_2-induced warming realized over an interval of time to the cumulative carbon emissions over that same time interval. This linear characterization provides a simplification suggested by Matthews et al. (2009) and others by targeting the composite response of the carbon and temperature dynamics instead of the components that induce it. MacDougall et al. (2017) provide a pedagogical summary of this literature and report a histogram for the TCRE computed for 150 model variants. Their histogram looks very similar to what we report in Figure 2.

Figure 1 shows the contribution of uncertainty in temperature and carbon dynamics to the temperature impulse responses. In generating the middle panel of Figure 1, we computed the implied temperature responses for nine alternative models of atmospheric CO_2 dynamics averaging over the seventeen models of temperature dynamics. In generating the lower panel of Figure 1, we

computed the seventeen temperature responses for seventeen temperature models while averaging over the nine models of atmospheric CO_2 dynamics. Consistent with the results reported by Ricke and Caldeira (2014), we find heterogeneity in the temperature responses to be more prominent than that coming from the atmospheric CO_2 dynamics.[3]

3 Damage uncertainty

We follow Barnett et al. in our construction of potential damage functions with specifications motivated by prior contributions. We posit a damage process, N_t, to capture negative externalities on society imposed by carbon emissions. The reciprocal of damages, $\frac{1}{N_t}$, diminishes the productive capacity of the economy because of the impact of climate change. We model the logarithm of damages as a function of changes in temperature induced by carbon emissions:

$$\log N_t = \Lambda \left(T_t - \underline{\tau} \right)$$

where $\underline{\tau}$ is pre-industrial temperature and Λ is piecewise quadratic

$$\Lambda(\tau) = \begin{cases} \lambda_1 \tau + \frac{\lambda_2}{2} \tau^2 & \tau \leqslant \overline{\tau} \\ \lambda_1 \tau + \frac{\lambda_2}{2} \tau^2 + \frac{\lambda_2^+}{2} \left(\tau - \overline{\tau} \right)^2 & \tau \geqslant \overline{\tau} \end{cases}$$

We let $\overline{\tau}$ equal a temperature anomaly of two degrees centigrade.

Barnett et al. consider two specifications of damages motivated by prior research. One specification sets $\lambda_2^+ = 0$ and sets λ_2 to approximate Nordhaus (2018). We refer to this as the low damage specification. A second specification sets $\lambda_2^+ > 0$ to capture the steeper degradation in damages that Weitzman (2012) argued for. We refer to this as the high damage specification. While Weitzman used uncertainty based on the potential fat tails in the posterior distribution for unknown damage coefficients, we follow Barnett et al. and introduce a high damage possibility and explore how a prudent decision maker should respond to the resulting damage function. We plot the high and low damage functions in Figure 3. Finally, there has been considerable discussion from the geo-sciences of the need to impose a two degree carbon budget. This corresponds to the vertical line in Figure 3. Rather than naively embrace this view, we introduce a third damage function that is much steeper than the high damage function reported in the figure for which there is a one third reduction in the productive capacity of the economy due to a three degree temperature increase.

[3] Ricke and Caldeira (2014) also consider separately two sources of temperature dynamics.

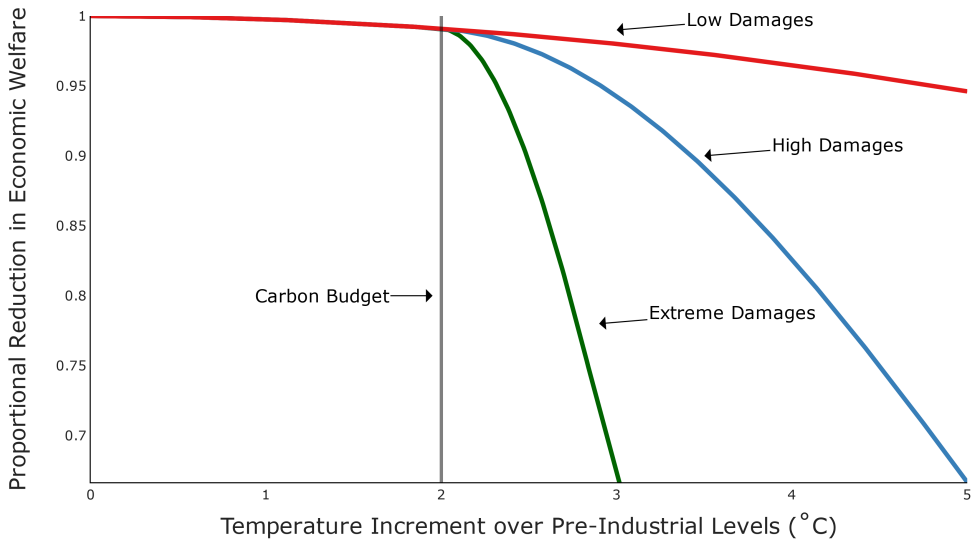

Figure 3: Three possible damage functions. This figure plots $\exp\left[-\Lambda(\tau)\right]$.

In our calculations so far, we have followed Barnett et al. by adopting the so-called "Matthews approximation." For the sake of illustration, we feature the exponential average response of temperature to emissions pulses when implementing this approximation. Call this parameter β. Specifically, we suppose that

$$T_t^d = \beta Y_t$$

where Y_t is cumulative emissions since pre-industrial times and thus satisfies:

$$dY_t = E_t dt$$

where E_t denotes the date t emissions flow. Then βY_t becomes the date t argument of the function Λ used to represent damages. While there are other reasons for temperature to fluctuate not linked to human CO_2 emissions, we think of βY_t as representing the human contribution to climate change.

This specification misses the initial build up in the temperature response and instead focuses exclusively on the flat trajectories depicted in the upper panel of Figure 1. In subsequent research we will explore formally how much we miss by in the SCC computations by overstating the initial temperature response. We expect that this error might be small when the prudent social planner embraces preferences that have a low rate of discounting the future. Armed with this "Matthews' approximation," we collapse the climate change uncertainty into the cross-model empirical distribution reported in Figure 2.

We now alter our construction of damages to be:

$$\log N_t = \Lambda\left(\beta Y_t\right) + \zeta_1(Z_t) Y_t + \zeta_2(Z_t)$$

with a stochastic evolution:

$$d\log N_t = \beta\left[\frac{d}{d\tau}\Lambda\right](\beta Y_t)E_t dt + \zeta_1(Z_t)\cdot E_t + d\zeta_1(Z_t)Y_t + d\zeta_2(Z_t) \tag{1}$$

where $\left[\frac{d}{d\tau}\Lambda\right]$ is the derivative of Λ with respect to its scalar argument and multiplication by β follows from the chain rule. We have included $\{[\zeta_1(Z_t), \zeta_2(Z_t)]\}$ to capture fluctuations in damages expressed as functions of an underlying diffusion process $\{Z_t\}$. This evolution for damages conditions on the specification of the coefficient β and economic damage specification Λ.

An important input into our SCC calculations is the impulse response function of future log damages to a current marginal change in emissions. This is an economically relevant "pulse experiment." From the dynamic evolution equation (1), this response function expressed as a function of the horizon u is

$$\underbrace{\left\{\beta\left[\tfrac{d}{d\tau}\Lambda\right](\beta Y_t) + \zeta_1(Z_t)\right\}}_{\text{direct effect}} \quad + \quad \underbrace{\left\{\beta^2\int_0^u \left(\left[\tfrac{d^2}{d\tau^2}\Lambda\right](\beta Y_{t+s})E_{t+s}\right)ds + \zeta_1(Z_{t+u}) - \zeta_1(Z_t)\right\}}_{\text{indirect effect}} \tag{2}$$

The first term does not depend on u and captures the (approximately) permanent direct impact of of emissions on future log damages, and the second term reflects the indirect impact as a change in emissions alters future values of the state variable Y_t.[4] This impulse response formula conditions on the model.

4 Economic model

To study the uncertainty on the SCC, we specify an illustrative economic model with adverse implications for climate change.

4.1 Technology

Abstracting from climate change, we use an AK model with adjustment costs. Capital evolves as:

$$dK_t = K_t\left[\mu_k(Z_t)dt + \phi_0\log\left(1+\phi_1\frac{I_t}{K_t}\right)dt + \sigma_k\cdot dW_t\right]$$

where $K_t\sigma_k\cdot dW_t$ is the component of a Brownian increment dW_t that captures randomness in the technology. The adjustment cost parameters satisfy: $0<\phi_0<1$, $\phi_1>1$. For computational purposes, it is convenient to write this in terms of logarithms:

$$d\log K_t = \mu_k(Z_t)dt + \phi_0\log\left(1+\phi_1\frac{I_t}{K_t}\right) - \frac{|\sigma_k|^2}{2}dt + \sigma_k\cdot dW_t$$

[4] Since the first derivative of $\Lambda(\tau)$ has a kink at $\tau=\overline{\tau}$ this formula breaks down at any time points for which $\beta Y_{t+s}=\overline{\tau}$.

Output is proportional to capital and split between consumption, C_t, and investment, I_t:

$$\alpha K_t = C_t + I_t.$$

Dividing through by K_t gives a computationally convenient expression of the controls relative to capital:

$$\alpha = \frac{C_t}{K_t} + \frac{I_t}{K_t}.$$

Climate change alters the productive capacity of the economy through scaling output by $\frac{1}{N_t}$. With this in mind, we define: $\widetilde{K}_t = \frac{K_t}{N_t}, \widetilde{C}_t = \frac{C_t}{N_t}$, and $\widetilde{I}_t = \frac{I_t}{N_t}$ where the $\tilde{\cdot}$ variables are damaged counterparts of the respective variables. Under this interpretation, climate change proportionately reduces output and alters the dynamic evolution of capital.

4.2 Preferences

We use discounted expected utility adjusted for model ambiguity aversion using the continuous-time formulation of Hansen and Miao (2018). The per period (instantaneous) contribution to preferences is:

$$\begin{aligned}
&\delta(1-\eta)\left(\log C_t - \log N_t\right) + \delta\eta \log E_t \\
&= \delta(1-\eta)\left[\log\left(\alpha - \frac{I_t}{K_t}\right) + \log K_t - \log N_t\right] + \delta\eta \log E_t \\
&\doteq U\left(\log K_t, \log N_t, E_t, \frac{I_t}{K_t}\right)
\end{aligned}$$

where $\log C_t - \log N_t = \log \widetilde{C}_t$ is the damaged-adjusted consumption, δ is the subjective discount rate, and $0 < \eta < 1$ measures the relative importance of emissions. We weight the instantaneous utility by the subjective discount rate for notational simplification in some derivations.

Remark 4.1. *A model that is mathematically equivalent is one in which we introduce a direct preference for not damaging the environment as captured by* $-\log N_t$ *and there is no loss in the productive capacity of the economy.*

4.3 Ambiguity aversion and robustness

In generating Figures 1 and 2 we gave equal weight to all 153 model configurations. Similarly, we assign equal weight to the high and low damage specifications given in Figure 3, except for some of our results where we entertain the possibility of the more extreme damage scenario. This gives us *ex ante* probabilities for the $J = 459$ discrete model specifications which we denote as $\pi_j^o : j = 1, ..., J$.

We explore the consequences of changing this weighting subject to a relative entropy penalty.

Entropy for a discrete set of probabilities, $\pi_j, j = 1, 2, .., J$ relative to an equal weighting is

$$\sum_{j=1}^{J} \pi_j \left(\log \pi_j - \log \pi_j^o\right)$$

where $\pi_j \geqslant 0$ and $\sum_{j=1}^{J} \pi_j = 1$. We multiply relative entropy by a penalty parameter ξ and include this in a recursive representation of a decision problem of a fictitious policy maker. By setting the penalty parameter to be arbitrarily large, we approximate a firm commitment to the equal weighting of the alternative specifications of the composite mapping of emissions to damages.

For the decision problem, we use the output constraint to substitute for consumption. We then let emissions and the investment-capital ratio be the choice variables denoted by e and i, respectively. The state vector, X_t, consists of log damages, $\log N_t$, log capital, $\log K_t$, cumulative carbon emissions, Y_t, and Z_t, which we use to model exogenous shifters of damages and capital evolution. We represent the composite state evolution as:

$$dX_t = \mu\left(X_t, E_t, \frac{I_t}{K_t}, j\right) dt + \sigma(X_t) dW_t$$

for model j where $j = 1, 2, ..., J$.

Let V denote a value function and U the instantaneous utility function. The Hamilton-Jacobi-Bellman (HJB) equation associated with our decision problem is:

$$\begin{aligned} 0 = \max_{e,i} \min_{\pi_j : \sum_{j=1}^{J} \pi_j = 1} & -\delta V(x) + U(x, e, i) + \frac{\partial V}{\partial x}(x) \cdot \sum_{j=1}^{J} \pi_j \mu(x, e, i, j) + \xi \sum_{j=1}^{J} \pi_j \left(\log \pi_j - \log \pi_j^o\right) \\ & + \frac{1}{2} \text{trace}\left[\sigma(x)' \frac{\partial^2 V}{\partial x \partial x'}(x) \sigma(x)\right]. \end{aligned} \tag{3}$$

An outcome of the minimization is a form of robustness in the choice of weights to assign to the various models. Given (e, i), there is a quasi-analytical formula for the π_j's:

$$\pi_j \quad \propto \quad \exp\left[-\frac{1}{\xi} \frac{\partial V}{\partial x}(x) \cdot \mu(x, e, i, j)\right] \pi_j^o$$

The probabilities tilt toward the μ's that adversely impact the local evaluation of the continuation-value process $\{V(X_t)\}$. In this sense, a planner facing ambiguity aversion slants probabilities toward models with adverse implications for the decision rules.

Remark 4.2. *We use the continuous-time formulation of ambiguity aversion proposed by Hansen and Miao (2018). It has two mathematically equivalent interpretations. One is a limiting version of the recursive specification of smooth ambiguity preferences of Klibanoff et al. (2009). The other is a robust adjustment to the decision-makers benchmark prior. Hansen and Sargent (2007) first noted this dual interpretation in a discrete-time setting. The robust prior interpretation extends to*

the continuous-time specification of Hansen and Miao and is used by Barnett et al. (2020) in their construction of an altered probability measure to use for valuation under model ambiguity.

The value function for this problem is additively separable in k (a potential realization of $\log K_t$) and n (a potential realization for $\log N_t$), which simplifies substantially our numerical calculations. Thus, we write:

$$V(x) = \upsilon_k k + \upsilon_n n + \widehat{V}(y, z)$$

From the HJB equation (3),

$$-\delta\upsilon_k + \delta(1-\eta) = 0$$
$$-\delta\upsilon_n - \delta(1-\eta) = 0$$

implying that $\upsilon_k = -\upsilon_n = (1-\eta)$. Moreover, as currently posed, the model ambiguity is only present in the drift specification for log damages and not for capital. The state variable y is effectively an "accounting variable" and also immune to model misspecification concerns.

Remark 4.3. *The mathematical separation of the logarithm of "undamaged capital" captured by the state k and the logarithm of damages captured in the HJB equation by d is computationally convenient. We are not, however, presuming an economic separation in the sense that k is a mathematical construct while the actual capital stock harmed by climate change is* $\exp(k-n)$*, when expressed in logarithms.*

Remark 4.4. *Barnett et al. (2020) included exploration for new reserves in their analysis. This enriched the technology and introduced an implicit production for emissions. This cost turns out to be quantitatively small relative to the social cost of carbon, leading us to drop exploration from the computations we report here for simplicity. In our view, a more important extension would include a green technology that becomes relatively more attractive as the social cost of carbon increases.*

The first-order conditions for e are:

$$\frac{\delta\eta}{e} - (1-\eta)\sum_{j=1}^{J}\left[\pi_j\beta_j\left[\frac{d}{d\tau}\Lambda_j\right](\beta_j y)\right] - (1-\eta)\zeta_1(z) + \frac{\partial\widehat{V}}{\partial y}(y,z) = 0, \tag{4}$$

which we will feature in our uncertainty decompositions that follow.

5 Uncertainty in the SCC

The problem facing the social planner posed as in HJB equation (3) gives us the SCC: it is the shadow price of emissions relative to consumption evaluated at the solution to the planner's problem. From the first-order conditions, (4), we obtain

$$\frac{\delta\eta}{e^*(y,z)} = (1-\eta)\sum_{j=1}^{J}\left[\pi_j^*(y,z)\beta_j\left[\frac{d}{d\tau}\Lambda_j\right](\beta_j y)\right] + (1-\eta)\zeta_1(z) - \frac{\partial\widehat{V}}{\partial y}(y,z) \tag{5}$$

where $e^*(x)$ is the maximizing decision rule for emissions and the $\pi_j^*(x)$'s are the state dependent minimizing probabilities. The two terms on the right-hand side reflect the expected discount values of the marginal utility of damages. The first captures what we referred to as the direct impact of emissions and the second one the indirect impact because emissions today have permanent consequences for future values of Y_t.

Barnett et al. quantify uncertainty with the difference of two discounted expected values, one using the probability measure imputed by the social planner that adjusts for ambiguity aversion and another that uses the baseline probability measure. We divide this difference by the marginal utility of damaged consumption to convert it into a social price.

5.1 Some social valuation accounting

For our uncertainty decompositions, we interpret the right-hand side of (5) as an expected discounted value of future marginal damages. First, we adjust the marginal damage responses in (2) by converting them into discounted marginal utilities by multiplying by $\delta(1-\eta)$. We complete the social accounting by exponentially discounting these marginal utilities at a rate δ, taking expectations, and integrating over u. Since the direct effect does not depend on the horizon u, it follows that

$$\begin{aligned}&\delta(1-\eta)\int_0^\infty \exp(-\delta u)\left(\beta\left[\frac{d}{d\tau}\Lambda\right](\beta Y_t)+\zeta_1(Z_t)\right)\\&=(1-\eta)\left(\beta\left[\frac{d}{d\tau}\Lambda\right](\beta Y_t)+\zeta_1(Z_t)\right)\end{aligned}$$

Applying integration-by-parts, we represent the discounted response for the indirect effect as[5]

$$\begin{aligned}&\delta(1-\eta)\int_0^\infty \exp(-\delta u)\left[\beta^2\int_0^u\left[\frac{d^2}{d\tau^2}\Lambda\right](\beta Y_{t+s})E_{t+s}ds+\zeta_1(Z_{t+u})-\zeta_1(Z_t)\right]du\\&=(1-\eta)\int_0^\infty \exp(-\delta u)\left(\beta^2\left[\frac{d^2}{d\tau^2}\Lambda\right](\beta Y_{t+u})E_{t+u}+\delta\zeta_1(Z_{t+u})\right)du-(1-\eta)\zeta_1(Z_t).\end{aligned}$$

Our uncertainty decompositions use different probabilities to compute expectations of these two contributions to the discounted impulse response function.

Let $\pi_j : j = 1, 2, ..., J$ denote probabilities over the discrete set of models. We will illustrate later the sensitivity of the SCC to uncertainty by exploring the consequences of different choices of model probabilities. In what follows, we spell out the steps for deriving the two contributions for the SCC for a given set of π_j's. Both are based on the marginal (social) value of emissions, ME, but with altered probabilities. To obtain the SCC from ME, we divide ME by the marginal

[5] For integration by parts, the derivative of one of the functions is $\delta\exp(-\delta u)$ and the other function is expressed as an integral between zero and u.

utility of damaged consumption, which gives the formula:

$$SCC(x) = ME(y,z)\frac{(\alpha - i^*)\exp(k-n)}{\delta(1-\eta)}$$

where i^* is the optimized investment capital ratio.

In our uncertainty decompositions, we compute ME in the following four steps:

i) compute

$$ME_1(y,z) = (1-\eta)\left(\sum_{j=1}^{J}\pi_j\beta_j\left[\frac{d}{d\tau}\Lambda_j\right](\beta_j y) + \zeta_1(z)\right);$$

ii) construct

$$U(y,z) = (1-\eta)\left[\sum_{j=1}^{J}\pi_j(\beta_j)^2\left[\frac{d^2}{d\tau^2}\Lambda_j\right](\beta_j y)e^*(y,z) + \delta\zeta_1(z)\right];$$

iii) solve

$$0 = -\delta f + \frac{\partial f}{\partial y}e^* + \frac{\partial f}{\partial z}\cdot\mu_z + \frac{1}{2}\text{trace}\left[(\sigma_z)'\left(\frac{\partial^2 f}{\partial z\partial z'}\right)\sigma_z\right],$$

which is a special case of a Feynman-Kac equation;

iv) compute $ME_2(y,z) = f(y,z) - (1-\eta)\zeta_1(z)$, and $ME(y,z) = ME_1(y,z) + ME_2(y,z)$.

We now consider alternative probabilities.

5.2 Planner ambiguity-adjusted probabilities

For the robust SCC^*, we let $\pi_j = \pi_j^*$ for $j = 1, 2, ...J$ where the latter probabilities are the penalized "worst-case" probabilities from the planner's problem.[6] By applying the "Envelope Theorem" we may show that

$$ME_2^* = -\frac{\partial\widehat{V}}{\partial y}.$$

where $\widehat{V}$ comes from solving the planner's HJB problem.

5.3 Baseline probabilities

To capture the overall impact of uncertainty, as a comparison we form SCC_o using the original baseline $\pi_j = \pi_j^o$ for $j = 1, 2, .., J$. Barnett et al. propose measuring the uncertainty component using

$$SCC^* - SCC^o.$$

We report this composite measure of uncertainty in Figure 4 for the special case in which $\zeta_1 = 0$,[7]

[6] These probabilities depend on the state y.

[7] We use the same parameter values as Barnett et al. (2020).

In this figure we assign benchmark probabilities to 356 model configurations. We assign probability of one half to high damages and low damages. A future draft of this paper will include the more extreme damage specification with a small probability. The nine carbon dynamic models are assigned marginal probabilities of one ninth each. The seventeen temperature are assigned marginal probabilities of one seventeenth each. The joint probabilities are given by the product of the marginals under the benchmark specification. These are the probabilities used in Figure 4. For the choice of ambiguity aversion used by Barnett et al. (2020), there is a sizeable contribution coming from probabilities adjusted for ambiguity aversion.

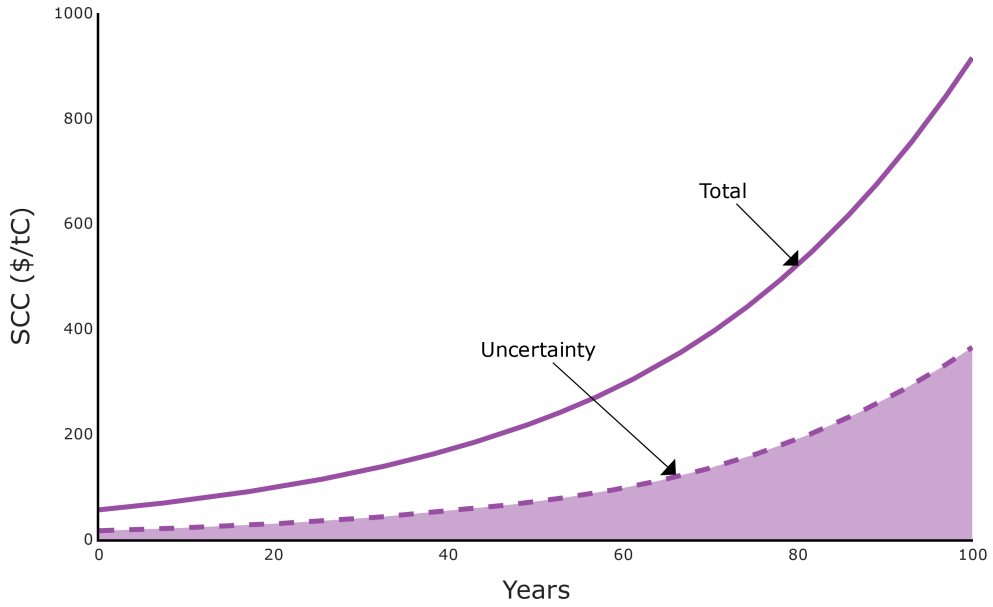

Figure 4: The overall contribution of uncertainty to the SCC. This plots the prospective SCC^* (labeled as *total*) and $SCC^* - SCC^o$ (labeled as *uncertainty*) over the next one hundred years. The units are in 2010 dollars.

5.4 Partitioning the uncertainty

The HJB equation in (3) also opens the door to some interesting additional uncertainty assessments. By restricting the distortion or minimization of the π_j's in alternative ways, we will deduce contributions to the SCC coming separately from uncertainty in i) temperature dynamics, ii) carbon dynamics, and iii) economic damage functions. This will allow us to understand better the most and least consequential sources of uncertainty as they pertain to climate change policy.

Let P_ℓ for $\ell = 1, 2, ...L$ be a partition of the positive integers up to J. Let J_ℓ denote the number of indices in partition P_ℓ. We will choose these partitions to correspond to alternative models of carbon dynamics, temperature dynamics, or damages functions either separately or in pairs.

Given any such partitioning, we compute the minimizing distorted probabilities $\overline{\pi}_\ell, \ell = 1, 2..., L$

for each of the partitions from the problem

$$
\begin{aligned}
0 = \min_{\overline{\pi}_\ell : \sum_{\ell=1}^{L} \overline{\pi}_\ell = 1} & -\delta V(x) + U[x, e^*(x), i^*(x)] \\
& + \frac{\partial V}{\partial x}(x) \cdot \sum_{\ell=1}^{L} \overline{\pi}_\ell \left(\frac{1}{\sum_{j \in P_\ell} \pi_j^o} \right) \sum_{j \in P_\ell} \pi_j^o \mu[x, e^*(x), i^*(x), j] \\
& + \xi \sum_{\ell=1}^{L} \overline{\pi}_\ell \left(\log \overline{\pi}_\ell - \log \overline{\pi}_\ell^o \right) + \frac{1}{2} \text{trace} \left[\sigma(x)' \frac{\partial^2 V}{\partial x \partial x'}(x) \sigma(x) \right] \qquad (6)
\end{aligned}
$$

Since minimization is involved, this is an HJB equation where we are holding fixed the conditional probabilities within each partition and change only the probabilities across partitions. This constraint on the probabilities is not imposed in the original HJB equation (3).

Given the special structure of our problem, the minimization is static in nature and the probabilities can be obtained by solving

$$
\begin{aligned}
\min_{\overline{\pi}_\ell : \sum_{\ell=1}^{L} \overline{\pi}_\ell = 1} & (\eta - 1) \sum_{\ell=1}^{L} \overline{\pi}_\ell \left(\frac{1}{\sum_{j \in P_\ell} \pi_j^o} \right) \sum_{j \in P_\ell} \pi_j^o \beta_j \left[\frac{d}{d\tau} \Lambda_j \right] (\beta y) e^*(y) \\
& + \xi \sum_{\ell=1}^{L} \overline{\pi}_\ell \left(\log \overline{\pi}_\ell - \log \overline{\pi}_\ell^o \right)
\end{aligned}
$$

Because of this structure, there is no need to compute the associated value function V. Call the minimizing probabilities for the partitions: $\overline{\pi}_\ell^p$ for $\ell = 1, 2, ...L$. Then form:

$$
\pi_j^p = \pi_j^o \frac{\overline{\pi}_\ell^p}{\overline{\pi}_\ell^o} \text{ for } j \in P_\ell,
$$

and denote the resulting SCC as SCC^p.

The upper panel of Figure 5 compares the outcome of three different partitions of a set of 356 model configurations. We form one partition for the temperature models, a second partition for the climate models and a third one for the damage models and assess their impact on the SCC by computing the corresponding SCC^p curves. We find, relatively speaking, the contribution of temperature dynamics to uncertainty in the SCC to be the largest and contribution of carbon dynamics to be the smallest. All three of the SCC^p curves are very close to that of SSC^o constructed using the baseline probabilities. Thus uncertainty contributed by each of the three components in isolation has little impact on the SCC. It is apparently the interaction of all three that is important.

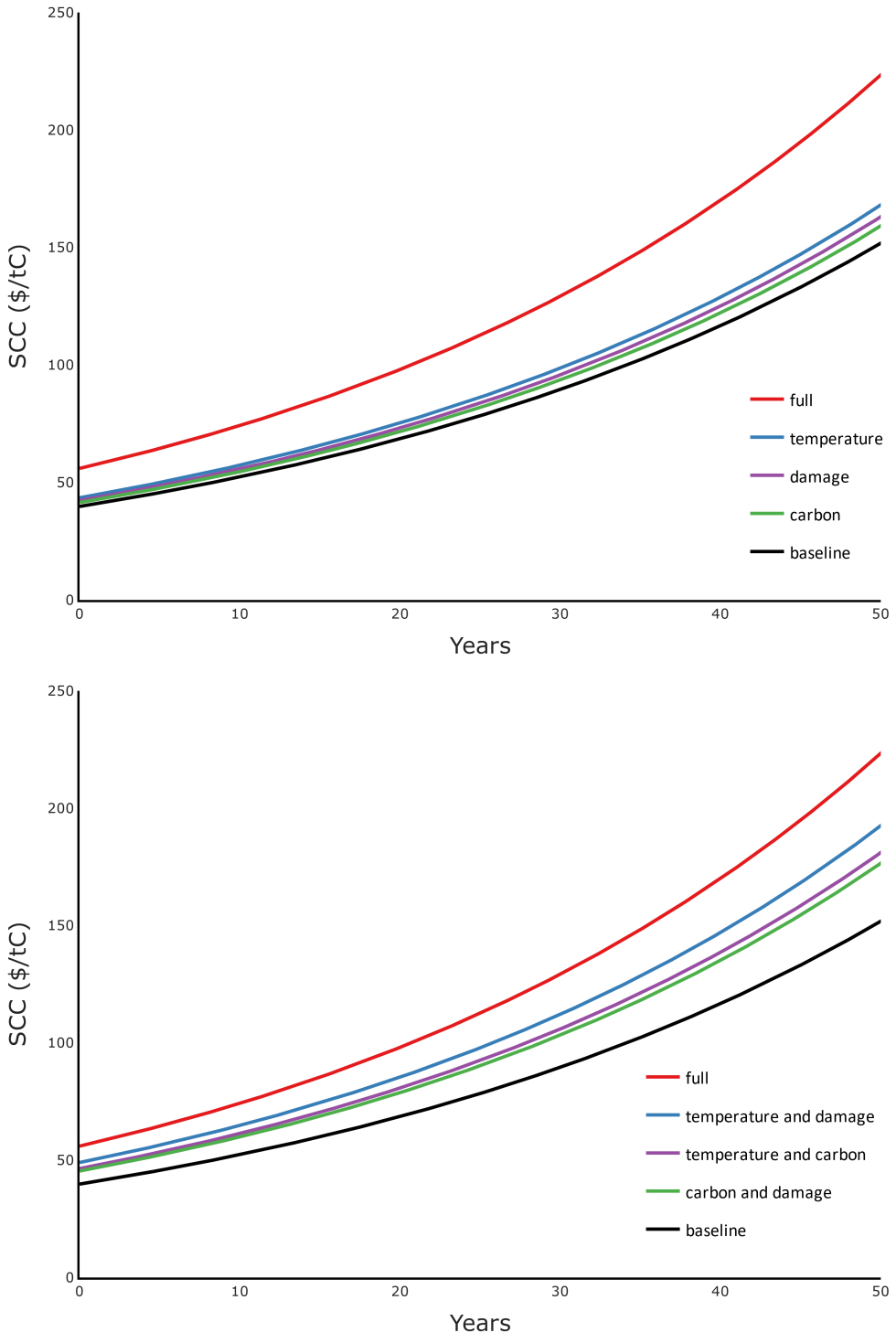

Figure 5: SCC uncertainty adjustments for alternative partitions. The upper panel partitions are constructed from the three different model components, and the lower panel partitions are constructed from the three alternative pairs of model components. For comparison, the upper red curve includes all three model components, and the bottom black curve uses the baseline probabilities.

This interaction is evident when we look at the lower panel of Figure 5. In this lower panel we construct a finer partition by combining two components of the three uncertainty components. Since there are three possible pairings, we report three versions of SSC^p. All three are now considerably higher than the baseline probability curve SSC^o. The highest of these curves features uncertainty in the combination of temperature dynamics and damage functions. The lowest SSC^p curve features uncertainty in the combination of carbon dynamics and damage functions. By comparing the upper and lower panels we see evidence of the multiplicative nature of the uncertain components. The uncertainty as captured by the lower panel of this figure shows, in particular, that uncertainty in temperature dynamics are substantial when we simultaneously consider uncertainty in the damage functions.

6 Caution induced by ambiguity aversion

An ambiguity averse planner in our environment expects to do less damage to economic opportunity through a lower choice of emissions in the future. We display this impact in Figure 6. Here we consider a planner who uses the baseline probabilities to one who is uncertain about how to weight the alternative models using the ambiguity aversion imposed in the previous section. The planner faces uncertain outcomes going forward because of ambiguity over how to weight the alternative models. This figure gives a range of possible damage outcomes. Across this range the ambiguity averse planner does notably less damage to productive capacity of the economy, but at cost of lower emissions. But even the ambiguity neutral planner only induces damages of about two percent after one hundred years under the lowest trajectory reported. This trajectory assumes that the high damage function in place along with a climate sensitivity parameter at the .9 quantile of the baseline set of probabilities. The possibility of a more extreme damage function could alter these numbers in a substantial way.

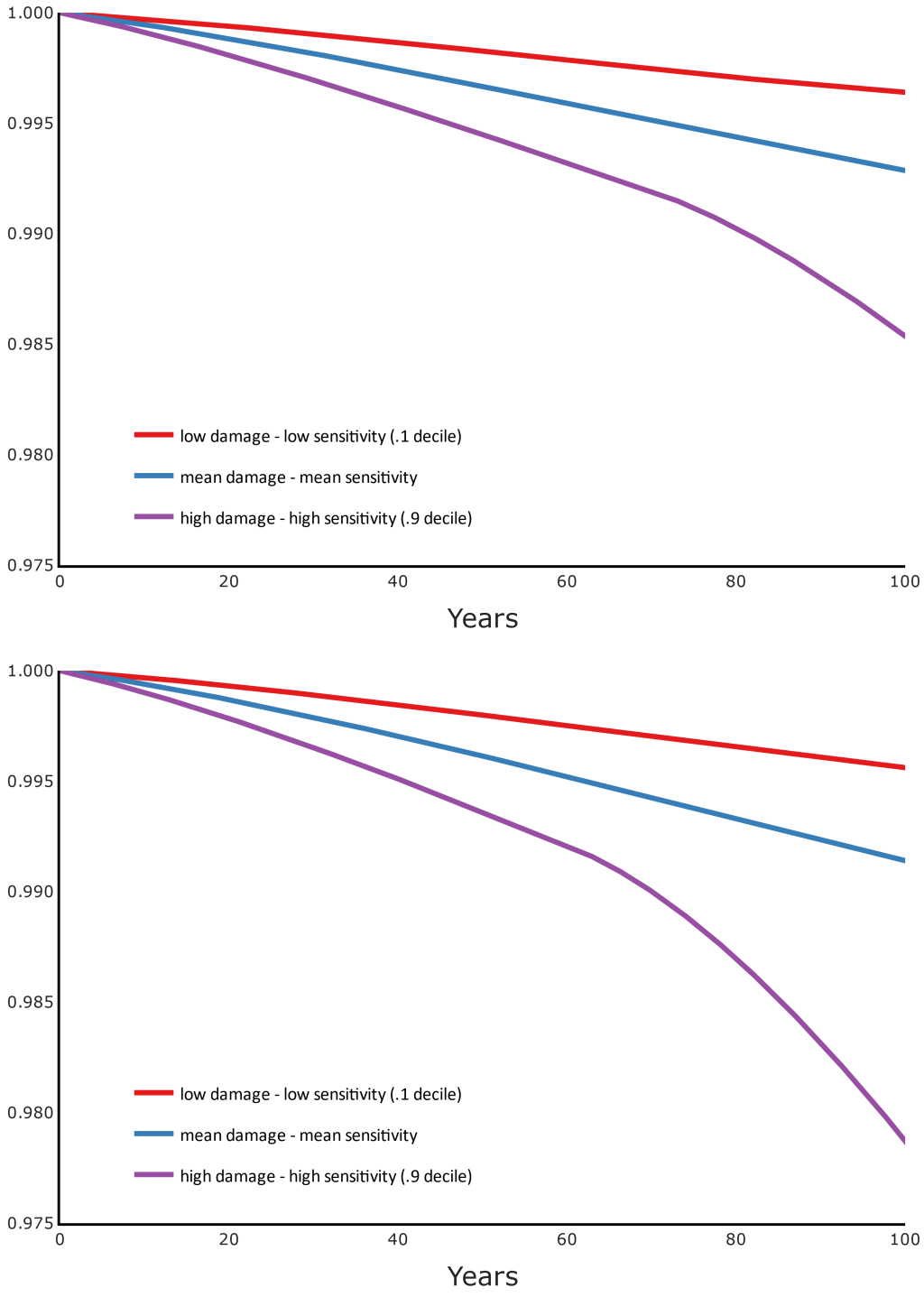

Figure 6: Damage uncertainty and aversion. The damages in the upper panel are constructed from the emission trajectory chosen by a social planner who is ambiguity averse. The three different damage curves are constructed from three different choices of climate sensitivity (.1 quantile, mean, and .9 quantile) coupled with the low damage function, the average damage function and the high damage function. The lower panel repeats this construction for when the social planner is ambiguity neutral.

Conclusion

An important step towards the design and implementation of effective climate policy is to understand and address the uncertainty in climate-economic models. Our analysis focuses on how different channels of uncertainty in a coupled climate economic system impact the socially optimal valuation of climate change costs. Recent papers such as Ricke and Caldeira (2014), Dietz et al. (2020), and others have begun to probe the importance of more complete climate models and their impact on the economic analysis of climate change. However, and importantly, we apply the tools of asset pricing and decision theory in an optimizing framework to characterize the impact of overall climate model uncertainty based on these more complex models, as well as decompose these effects by model component to demonstrate the relative importance of uncertainty along each channel.

Our decomposition analysis focuses on three dynamic mappings in the path between carbon emissions and futures damages to the economy: (i) carbon emissions to carbon content in the atmosphere, (ii) carbon content in the atmosphere to global temperature, (iii) and global temperature to damages to the world economy. The decompositions use piecewise constrained robustness for different partitions created using a quantitatively disciplined multiple geoscientific model framework for channels (i) and (ii), and supplemented by a small number of quantitatively disciplined economic damage functions for channel (iii). Importantly, the resulting valuations allow us to identify which of the three uncertainty channels, or combinations of subsets of the three channels, are likely to be most relevant in terms of their relative impact on the SCC and for climate policy action. We believe this to be the first uncertainty decomposition of its kind in the literature, and that similar uncertainty decompositions may be of wider interest to many other settings of social valuation and policy analysis.

References

Barnett, Michael, William A. Brock, and Lars Peter Hansen. 2020. Pricing Uncertainty Induced by Climate Change. *Review of Financial Studies* 33 (3):1024–1066.

Cai, Yongyang, Kenneth L. Judd, and Thomas S. Lontzek. 2017. The Social Cost of Carbon with Climate Risk. Tech. rep., Hoover Institution, Stanford, CA.

Dietz, Simon, Rick van der Ploeg, Armon Rezai, and Frank Venmans. 2020. Are economists getting climate dynamics right and does it matter? .

Geoffroy, O, D Saint-Martin, D J L Olivié, A Voldoire, G Bellon, and S Tytéca. 2013. Transient Climate Response in a Two-Layer Energy-Balance Model. Part {I}: Analytical Solution and Parameter Calibration Using CMIP5 AOGCM Experiments. *Journal of Climate* 26 (6):1841–1857.

Golosov, Mikhail, John Hassler, Per Krusell, and Aleh Tsyvinski. 2014. Optimal Taxes on Fossil Fuel in General Equilibrium. *Econometrica* 82 (1):41–88.

Hansen, Lars Peter and Jianjun Miao. 2018. Aversion to Ambiguity and Model Misspecification in Dynamic Stochastic Environments. *Proceedings of the National Academy of Sciences* 115 (37):9163–9168.

Hansen, Lars Peter and Thomas J. Sargent. 2007. Recursive Robust Estimation and Control without Commitment. *Journal of Economic Theory* 136 (1):1–27.

Joos, F., R. Roth, J. S. Fuglestvedt, G. P. Peters, I. G. Enting, W. Von Bloh, V. Brovkin, E. J. Burke, M. Eby, N. R. Edwards, T. Friedrich, T. L. Frölicher, P. R. Halloran, P. B. Holden, C. Jones, T. Kleinen, F. T. Mackenzie, K. Matsumoto, M. Meinshausen, G. K. Plattner, A. Reisinger, J. Segschneider, G. Shaffer, M. Steinacher, K. Strassmann, K. Tanaka, A. Timmermann, and A. J. Weaver. 2013. Carbon Dioxide and Climate Impulse Response Functions for the Computation of Greenhouse Gas Metrics: A Multi-Model Analysis. *Atmospheric Chemistry and Physics* 13 (5):2793–2825.

Klibanoff, P, M Marinacci, and S Mukerji. 2009. Recursive {Smooth} {Ambiguity} {Preferences}. *Journal of Economic Theory* 144:930–976.

MacDougall, Andrew H., Neil C. Swart, and Reto Knutti. 2017. The Uncertainty in the Transient Climate Response to Cumulative CO_2 Emissions Arising from the Uncertainty in Physical Climate Parameters. *Journal of Climate* 30 (2):813–827.

Matthews, H Damon, Nathan P Gillett, Peter A Stott, and Kirsten Zickfeld. 2009. The proportionality of global warming to cumulative carbon emissions. *Nature* 459 (7248):829–832.

Morgan, M. Granger, Parth Vaishnav, Hadi Dowlatabadi, and Ines L. Azevedo. 2017. Rethinking the Social Cost of Carbon Dioxide. *Issues in Science and Technology* 33 (4).

Nordhaus, William. 2015. Climate clubs: Overcoming free-riding in international climate policy. *American Economic Review* 105 (4):1339–1370.

———. 2018. Projections and uncertainties about climate change in an era of minimal climate policies. *American Economic Journal: Economic Policy* 10 (3):333–360.

Pindyck, Robert S. 2013. Climate Change Policy: What Do the Models Tell Us? *Journal of Economic Literature* 51 (3):860–872.

Ricke, Katharine L. and Ken Caldeira. 2014. Maximum Warming Occurs about One Decade After a Carbon Dioxide Emission. *Environmental Research Letters* 9 (12):1–8.

Seshadri, Ashwin K. 2017. Fast–slow climate dynamics and peak global warming. *Climate Dynamics* 48 (7-8):2235–2253.

Wagner, Gernot and Martin Weitzman. 2015. *Climate Shock*. Princeton University Press.

Weitzman, Martin L. 2012. GHG Targets as Insurance Against Catastrophic Climate Damages. *Journal of Public Economic Theory* 14 (2):221–244.

Appendix A Carbon and Temperature Model Sets

As mentioned previously, we use 17 models of temperature dynamics from Geoffroy et al. (2013) and 9 models of carbon dynamics models from Joos et al. (2013). We briefly describe the model experiements used in these papers, list the models we include in our analysis, and provide details for the reader to find additional information about these models and model experiments.

Geoffroy et al. (2013) uses a two-layer energy-balance model (EBM) to study properties of atmosphere-ocean general circulation models (AOGCMs). Their EBM model is solved for explicit solutions, calibrated to fit the responses of 16 AOGCMs that participated in the CMIP5, and then validated by using the AOGCM responses to the linear forcing experiments of one percent of CO_2 per year. In addition, we include the model calibration from Seshadri (2017), which is based on the multi-model mean of Geoffroy et al. (2013). We list the model name for each of the models used in our analysis in Table 1 below. We direct the reader to Geoffroy et al. (2013) and Seshadri (2017) for additional details on the models.

Joos et al. (2013) use a carbon cycle-climate model intercomparison analysis to study the impulse response time-scales of Earth System models. From their analysis, we use the impulse response functions of 9 models based on a 100GtC emission pulse added to a constant CO_2 concentration of 389 ppm.[8] All of the models we use are Earth System Models of Intermediate Complexity, except for the reduced form model Bern-SAR. We list the model name for each of the models used in our analysis in Table 2 below. We direct the reader to Appendix A in Joos et al. (2013) for detailed descriptions of these and other models used in their model intercomparison analysis.

[8] We acknowledge Fortunat Joos for graciously providing the data for these and other response experiments on his website: https://climatehomes.unibe.ch/~joos/IRF_Intercomparison/results.html.

Temperature Dynamics Models
BCC-CSM1–1
BNU-ESM
CanESM2
CCSM
CNRM-CM5
CSIRO-Mk3.6.0
FGOALS-s2
GFDL-ESM2M
GISS-E2-R
HadGEM2-ES
INM-CM4
IPSL-CM5A-LR
MIROC
MPI-ESM-LR
MRI-CGCM3
NorESM1-M
Seshadri (2017)

Table 1: List of 17 temperature dynamics models from Geoffroy et al. (2013) and Seshadri (2017) used in our analysis.

Carbon Dynamics Models
Bern3D-LPJ (reference)
Bern2.5D-LPJ
CLIMBER2-LPJ
DCESS
GENIE (ensemble median)
LOVECLIM
MESMO
UVic2.9
Bern-SAR

Table 2: List of 9 carbon dynamics models from Joos et al. (2013) used in our analysis.